ACCSCIENCE PUBLISHING
An International Journal of Optimization and Control: Theories & Applications
ISSN: 2146-0957 eISSN: 2146-5703
Vol.15, No.4, pp.578-593 (2025)
https://doi.org/10.36922/IJOCTA025110050
IJOCTA

RESEARCH ARTICLE

Nonlinear image processing with α-tension field: A geometric approach

Seyyed Mehdi Kazemi Torbaghan[1], Yaser Jouybari Moghaddam[2], and Amin Jajarmi[3,4*]

[1]Department of Mathematics, University of Bojnord, Bojnord, Iran
[2]Department of Surveying Engineering, University of Bojnord, Bojnord, Iran
[3]Department of Electrical Engineering, University of Bojnord, Bojnord, Iran
[4]Department of Mathematics, Saveetha School of Engineering, Saveetha Institute of Medical and Technical Sciences, Saveetha University, Chennai,Tamil Nadu, India
m.kazemi@ub.ac.ir, a.jajarmi@ub.ac.ir, jouybari@ub.ac.ir

ARTICLE INFO

Article History:
Received: March 13, 2025
1st revised: March 27, 2025
2nd revised: May 3, 2025
3rd revised: May 16, 2025
Accepted: May 22, 2025
Published Online: June 6, 2025

Keywords:
Image processing
$\alpha-$tension field
Harmonic maps
Riemannian geometry

Subject Classification:
68U10;53C43; 58E20,

ABSTRACT

In this paper, we apply an α-tension field from differential geometry to classical image processing tasks of denoising with edge preservation and multiphase feature enhancement. The main contribution of this work is that it is the first systematic investigation of the α-tension field for image processing. Contrary to traditional operators, such as the Laplacian, which are susceptible to noise amplification or are ineffective for complex structures, the α-tension field relies on a nonlinear adaptive mechanism depending on the magnitudes of local gradients. It allows effective denoising and retains edges and fine details by utilizing higher-order gradient information. The field of α-tension provides more sensitive and adaptive models than linear models, such as total variation regularization, anisotropic diffusion, etc. The study exemplifies its advantages over previous methods in preserving structural integrity and minimizing artifacts. It also considers numerical implementation issues and provides guidelines for real-time and large-scale processing. This framework adds up to the known need for faster image-processing tools while links connections to differential geometry.

1. Introduction and background

The tension field is one of the important analytic and geometric objects to study in the context of harmonic mappings between Riemannian manifolds. For a smooth map $u : (M, g) \longrightarrow (N, h)$, we define the tension field of u to be the trace of the second fundamental form of u, so that $\tau(u) = \text{trace}g\nabla du$, where ∇ is the induced connection on $u^{-1}TN$.[1] Harmonic maps are, therefore, critical points of the energy functional, and they satisfy the Euler-Lagrange equation $\tau(u) = 0$. Nevertheless, the non-coercivity of the standard energy functional frequently adds technical difficulties to the existence theory for harmonic maps. To tackle this problem, Karen Uhlenbeck and Jonathan Sacks introduced the α-tension field,[2] which corresponds with the α-energy functional $E_\alpha(u) = \int_M (1+ \mid du \mid^2)^\alpha dvol_g$, for $\alpha > 1$. This approach guarantees connectivity, and it is used to build geometric objects called α-harmonic maps which are defined as the maps with vanishing α-tension field. These α-harmonic maps are used to construct the standard harmonic maps in the limit $\alpha \to 1$.[2]

The work of Karen Uhlenbeck on $\alpha-$tension field addresses fundamental questions regarding the existence and regularity of harmonic maps

*Corresponding Author

and gives important information for understanding a variety of phenomena (e.g., bubble formation), which are crucial for the understanding of singular behavior in many geometric variational problems.[1,3] She has made lasting contributions across geometry, analysis, and mathematical physics, winning the Abel Prize in 2019. All of her research is continuing to inspire new generations of mathematicians, providing not only deep theoretical understanding but also practical tools to tackle problems in the study of differential geometry and many related areas.

The concepts of α-tension fields and α-harmonic maps were recently studied extensively.[1,3–6] Several works[1,6] have dealth with dealt with the stability and existence of α-harmonic maps and the instability of non-constant α-harmonic maps in terms of the Ricci curvature of the target space as well as the determination of the Morse index to measure the degree of instability for certain maps. The notion of Sacks-Uhlenbeck α-harmonic maps was generalized to the Finsler space in Ref.[3], and it is also proved that any non-constant α-harmonic maps from a compact Finsler manifold to a standard unit sphere S^n $(n > 2)$ are unstable if some conditions hold. Moreover, in ref.,[5] the energy identity and necklessness of a blow-up sequence of α-harmonic maps was studied in the case when their codomain is the sphere S^{k-1}. This analysis gave an alternative proof of Perelman's theorem[7] that the Ricci flow of the compact orientable 3-dimensional manifold is extinct in finite time, which is profoundly different from the conclusion in ref.[4]

The use of the α-tension field, a concept from differential geometry, represents a substantial improvement over traditional operators such as the tension field operator and total variation regularization. Conventional methods have noise amplification, oversmoothing of detail, or the staircasing effect. The α-tension field does not suffer from these pitfalls; it utilizes higher-order gradients and geometric variational principles to balance its denoising, edge-preserving, and feature-enhancing capabilities. The nonlinear adaptive diffusion of the α-tension field is governed based on local image geometry, making it potentially very valuable for applications that require structures to remain intact, such as medical images. The α-tension field is responsive and sensitive to local gradient magnitudes to a larger degree than linear models permitting adaptiveness, allowing it to preserve edges and small features while denoising areas of smooth gradients. There are some numerical challenges to implement in practical, large-scale images, but commonly used techniques such as finite differences and iterative methods imply computations can remain efficient as well as numerically stable.

In this study, there is a multi-faceted benchmarking process involving advanced statistical analyses specifically directed toward the lung CT images for cancer detection in the LIDC-IDRI Dataset.[8] The performance metrics of interest (Structural Similarity Index [SSIM]) emphasizes the improvement in edge retention and noise suppression. This is particularly pertinent when compared against baseline methodologies, such as total variation regularization and anisotropic diffusion. The $\alpha-$tension field can circumvent many issues, such as oversmoothing, while also extending to other types of images and noise levels, proving effective in a number of tasks (e.g., satellite and medical imaging). Although computational complexity is limited, especially with regards to real-time situations, adaptive discretization schemes, and parameter tuning using machine learning methods can address real-time efficiency and image quality. Addressing these trade offs in the $\alpha-$tension field for a real-time integration holds valuable potential, and being able to utilize speed and precision as its own futuristic application in itself (i.e., virtual and augmented reality).

The research gap addressed in this paper lies in the lack of systematic exploration of the α-tension field, which is a differential geometry concept for image processing purposes. Classic operators (e.g., the Laplacian) and techniques (e.g., total variation regularization, anisotropic diffusion, etc.) often suffer from noise propagation, the oversmoothing of complex structures, and the so-called "staircasing" effect (especially in homogeneous regions), preventing them from effectively balancing denoising, edge preservation, and feature enhancement. This paper seeks to fill this void by presenting the α-tension field, a nonlinear adaptive system that regulates diffusion according to the local magnitudes of gradients, thus enforcing the retention of detail while reducing noise. In particular, the paper studies the case $\alpha = 2$, showing that it outperforms classical approaches via theoretical comparisons and empirical applications.

The key novelty of this work is the first application of the α-tension field, originally developed for harmonic mapping of Riemannian manifolds, to key challenges of image processing, such as edge detection, denoising, and shape enhancement. No other work has examined the applicability of α-tension fields for image processing tasks, and thus

this is the first study to systematically investigate the potential of the α-tension fields on image processing tasks. The proper noise smoothing, as well as, sharp feature extraction capabilities of the α-tension field, stems from its exploitation of higher-order gradient information in addition to being derived from geometric variational bases as opposed to classical linear operators, which either overly enhance the noise in the minimization process or prevent significant image details from being evident. As such, it presents a mathematically principled and generalizable framework for advanced image processing applications, including denoising, edge-preserving smoothing, and feature enhancement. Additionally, the authors integrate geometrical theory with the following practical implementations: this not only encourages more efficient image-analysis processes but also sets the stage for future inquiry into real-time and large-scale image-processing techniques.

This work differs from Ref.[9] in terms of theoretical contributions, methodologies, and novel applications. The paper[9] defines (α, f)-harmonic maps and checks how stable they are under different geometric conditions, like Ricci and sectional curvatures. However, it does not use these ideas in real-world image-processing tasks, so there is a gap between theory and practice. On the other hand, our manuscript addresses this limitation by proposing the 2-tension field ($\alpha = 2$) as a novel operator for image processing at the intersection of geometric theory and tangible applications. We use adaptive local gradient adjustments and finite difference methods to discretize the 2-tension field. This works around the problems that traditional operators (like Laplacian) have with being too smooth while keeping structural details. In addition, our work analyzes advanced applications like image denoising, edge preservation, and feature enhancement, which were not present in the literature.[9]

The rest of this paper is organized as follows: Section 2 gives a general description of the geometry of tension fields, generalizations of the geometry of tension fields, and there we introduce the α-tension field. It explores the mathematical underpinnings of these concepts and their role in geometric variational problems. Section 3 discusses the use of tension fields to handle certain problems in image processing, including edge detection, denoising, and local contrast enhancement. Section 4 is devoted to the utility of the α-tension field $\tau_\alpha(I)$ in image processing, emphasizing its benefits in denoising, edge preservation, and feature enhancement over conventional approaches. This leads us to Section 5, where the tension field and α-tension field are contrasted in both mathematical formulation and properties, as well as in practice. Finally, Section 6 summarizes the paper, noting implications and directions for future work.

2. Geometry of tension fields and α-tension fields

The tension field is a fundamental notion in geometric variational problems, which rely on the principles of energy minimization to study the structure of mappings between manifolds. These are rooted in differential geometry and yield strong results on how curvature, topology, and energy functionals restrict the behavior of mappings. This part has been dedicated to exploring the geometric background under tension fields and their generalizations, which we call $\alpha-$ tension fields. We emphasize their intrinsic mathematical features and discuss how these notions shed light on the relationship between energy minimization and the geometrical structure of mappings.

Let M and N be smooth Riemannian manifolds, M compact and oriented, and let $u : M \longrightarrow N$ be a smooth map. We can write the energy functional of u as:

$$E(u) = \frac{1}{2}\int_M \mid du \mid^2 \, dvol_g, \tag{1}$$

where $\mid du \mid^2$ is the norm of du with respect to the metrics on M and N, and $dvol_g$ is the volume form on M. Critical points of $E(u)$ are called harmonic maps, and they solve the Euler – Lagrange equation:

$$\tau(u) := \text{trace} g\nabla du = 0, \tag{2}$$

where ∇ is the induced connection on the pullback bundle $u^{-1}TN$, trace_g is the trace with respect to the metric g on M and $\tau(u)$ is the tension field of u.[7] Noting that the tension field measures the distance of u from a totally geodesic map.[5]

Geometrically, the tension field describes the amount of unbalance or stress in the map u. This reflects the dependence of how the geometry of the domain manifold M interacts with the geometry of the target manifold N. Specifically:

1. If $\tau(u) = 0$. The mapping u is harmonic, that is, it satisfies the condition that minimizes the energy functional, so that the tension is balanced at all points.[5]
2. The points where $\tau(u) \neq 0$ represent the regions where the map is either stretching or compressing excessively. These areas typically correspond to locations with high curvature or substantial variations in the mapping.[4]

Let $\alpha > 1$ be a constant. Given a map u, we define the α-energy functional of u by:

$$E_\alpha(u) := \int_M (1+ \mid du \mid^2)^\alpha dvol_g. \tag{3}$$

Hence, the critical points of E_α are α-harmonic maps. The Euler–Lagrange equation related to the α-energy functional E_α comes from applying Green's theorem:

$$\begin{aligned}\tau_\alpha(u) : &= (1+ \mid du \mid^2)^{\alpha-1}\tau(u) \\ &+ (\alpha-1)(1+ \mid du \mid^2)^{\alpha-2}\nabla I(\nabla \mid \nabla I \mid^2) \\ &= 0.\end{aligned} \tag{4}$$

The section $\tau_\alpha(u)$ is called the α-tension field of u.[2] We can then classify the main properties of the α-tension fields as

(1) Nonlinearity: Unlike the classical tension field, $\tau_\alpha(u)$ is intrinsically nonlinear as it contains terms of the powers of $\mid du \mid$. This nonlinearity creates new difficulties for the analysis of the existence and regularity of solutions.[2]
(2) Dependence on scaling: The factor $(1+ \mid du \mid^2)^{\alpha-1}$ causes $\tau_\alpha(u)$ to depend on the scaling of du. Indeed, the small-gradient maps are treated differently from the large-gradient maps in $\alpha-$energy functional.[3,6]
(3) Geometric flexibility: Varying α allows one to interpolate between different regimes of energy minimization, making it α flexible tool for the study of mappings between manifolds.[1]

Using Equations (3) and (4), we obtain the result:

Theorem 1. *[6] Let $u : (M, g) \longrightarrow (N, h)$ be a smooth map between Riemannian manifolds. Then u is α-harmonic if and only if its α-tension field vanishes.*

This is something analogous to the famous fact that α-harmonicity is equivalent to α-tension field vanishing.

Example 1. *Let $\alpha = 2$ and let $u : \mathbb{R}^2 \longrightarrow \mathbb{R}^3$ be a smooth map defined by:*

$$u(x_1, x_2) = (3x_2 - x_1, x_2 - 2x_1, 5x_2 + 3x_1). \tag{5}$$

By (4) and Theorem 1, it can be checked that u is an α-harmonic map

We show an explicit relation between the α-harmonic maps and the harmonic maps by conformal deformation:

Theorem 2. *[1] Any smooth map $u : (M^m, g) \longrightarrow (N^n, h)$ is an α-harmonic map if and only if it is harmonic with respect to the metric $\bar{g}$ conformally related to g given by:*

$$\bar{g} = \{(2\alpha)^{\frac{2}{m-2}}(1+ \mid du \mid^2)^{\frac{2\alpha-2}{m-2}}\}g. \tag{6}$$

Theorem 2 states an equivalence between α-harmonicity and the harmonicity of u with respect to a suitably conformally rescaled domain metric. The next theorem states the conditions for the existence of $\alpha-$harmonic maps in every homotopy class.

Theorem 3. *[1] Let $u : (M^m, g) \longrightarrow (N^n, h)$ be a harmonic map, and $\mathcal{H}$ be a homotopy class of u. Then, there is a smooth metric $\bar{g}$ on M conformally equivalent to g such that $u : (M, \bar{g}) \longrightarrow (N, h)$ is $\alpha-$harmonic for $m > 2\alpha$.*

The theme of tension fields and their generalizations, e.g., α-tension fields, has a deep geometrical interpretation rooted in the balance of energy and the local properties of maps, as manifested through geometry on manifolds. Although the classical tension field incorporates the behavior of harmonic maps, the α-tension field generalizes this concept to a more general set of variational problems. A manifold endowed with an additional structure (distance, metric, curvature, etc.) can facilitate the drawing of inferences on the properties of physical systems underpinning these mathematical constructs. The α-tension field introduces a parameterized family of tension fields and is a flexible and mathematically potent tool to tackle questions across geometry, analysis, and topology.

3. Application of tension fields in image processing

The concept of the tension field is the foundation for the mappings between Riemannian manifolds have been widely used in image processing. Here, we will explore these ideas and how they are applied in image analysis. The tension field is a link between geometry and optimization, allowing for advanced techniques in image processing.

Tension field has been widely adapted to show its relevance to possible applications in image processing, where an image can be seen as a function from a domain (e.g., a 2D image) to a codomain (e.g., pixel intensity values). Denote a 2D image by $I(x, y)$. By (4), the tension field of I, given by $\tau(I) = \text{trace}_g \nabla dI$, yields the simplification:

$$\tau(I) = \Delta I, \tag{7}$$

where $\Delta I := \frac{\partial^2 I}{\partial x^2} + \frac{\partial^2 I}{\partial y^2}$, is the Laplacian operator applied on the input image.[10] Computations

for the components of the gradient $\frac{\partial I}{\partial x}$ and $\frac{\partial I}{\partial y}$ using central difference approximations are done as follows[11]:

$$\frac{\partial I}{\partial x} \approx \frac{I(x+1,y) - I(x-1,y)}{2}, \\ \frac{\partial I}{\partial y} \approx \frac{I(x,y+1) - I(x,y-1)}{2}. \tag{8}$$

These derivative approximations can be expressed as convolution kernels in the filter form as:

$$\frac{\partial I}{\partial x} = \frac{1}{2}\begin{bmatrix} -1 & 0 & 1 \\ -1 & 0 & 1 \\ -1 & 0 & 1 \end{bmatrix}, \tag{9}$$

and:

$$\frac{\partial I}{\partial y} = \frac{1}{2}\begin{bmatrix} -1 & -1 & -1 \\ 0 & 0 & 0 \\ 1 & 1 & 1 \end{bmatrix}. \tag{10}$$

Similarly, the Laplacian ΔI is approximated by:

$$\Delta I \approx I(x+1,y) + I(x-1,y) + I(x,y+1) \\ + I(x,y-1) - 4I(x,y), \tag{11}$$

for more details, see.[11,12] Using (7) and (11), the filter associated with the tension field $\tau(I)$ is given by:

$$\tau(I) = \begin{bmatrix} 0 & 1 & 0 \\ 1 & -4 & 1 \\ 0 & 1 & 0 \end{bmatrix}. \tag{12}$$

As this kernel consists of a tension field that is very computationally efficient and compact, it may be easily adapted in a great many other image processing applications without sacrificing the basic geometric and analytical idea of the original tension field concept.[13]

The major applications of tension field can be mentioned as follows:

1. Edge detection: The tension field is widely used in edge detection because the edge indicates where the second derivative of an image intensity changes significantly. Edges reflect zero-crossings of this tension field (useful for detecting the discontinuities that separate two objects/regions).[14]
2. Image sharpening: The tension field sharpens the image by amplifying high-frequency components like edges and finer details. We do this by adding a scaled version of the tension field back to the original pixel image:

$$I_{\text{sharp}} = I + c\tau(I), \tag{13}$$

where $c > 0$ controls the intensity of the sharpening effect.[15]
3. Image smoothing: Although the tension field itself is noise-sensitive, its negative counterpart can be employed for smoothing by simply subtracting the high-frequency components:

$$I_{\text{smooth}} = I - c\tau(I). \tag{14}$$

However, this is less common than other smoothing techniques (e.g., Gaussian filtering) due to potential artifacts.[15]

4 Texture analysis: Breaks down an image into low-frequency and high-frequency components that can be found useful for texture pattern analysis. By analyzing how these components are spatially arranged/distributed, textures can be classified or even material properties can be identified.[16]

5 Image segmentation: The tension fields accentuate areas of rapid intensity change, serving as antecedent seeds for segmentation algorithms, for example, region-growing or level-set methods. The boundaries are usually aligned with object boundaries or different parts in the image.[17]

The tension field operator has a variety of applications in image processing, one of which is demonstrated in Figure 1. The left part of the figure illustrates the input image, which is the image of "Lena"one of the most popular references in image processing as it consists of many details and textures. The resulting image of the tension field as an operator to the input image is shown in the right part of the figure. This process, known as edge detection, computes the tension field of the image, accentuating areas of rapid intensity change (e.g., edges and boundaries). This gives an output which retains these characteristics (while smoothing out homogeneous areas), showing the representation and extraction power of the tension field on the image of its interesting structural information. Such examples showcase how functional the tension field can be both in enhancing as well as analyzing the image, thus serving as an efficiency tool for tasks like edge detection, denoising, and feature extraction.

Figure 1. The image on the left is the original, whereas the image on the right demonstrates the effect of the tension field on the original image.

Algorithm 1 Tension field algorithm for Figure 1

procedure TensionField(*Image*)
  Input: *Image* (2D array), **Output:** *Result*
  Initialize *Result* with zeros, same size as *Image*
  Kernel $\leftarrow \begin{bmatrix} 0 & 1 & 0 \\ 1 & -4 & 1 \\ 0 & 1 & 0 \end{bmatrix}$
  for $i = 1$ to $rows - 2$ **do**
    for $j = 1$ to $cols - 2$ **do**
      $Sum \leftarrow 0$
      for $m = 0$ to 2 **do**
        for $n = 0$ to 2 **do**
          $Sum \mathrel{+}= Kernel[m][n] \times Image[i - 1 + m][j - 1 + n]$
        end for
      end for
      $Result[i][j] \leftarrow Sum$
    end for
  end for
  return *Result*
end procedure

The algorithm used in Figure 1 to apply the tension field and demonstrate its effect is presented in Algorithm 1. This algorithm outlines the steps involved in computing the tension field and illustrates how it is applied to achieve the desired outcome depicted in Figure 1.

As we have seen in this section, the tension field is the fundamental concept in the study of mappings between Riemannian manifolds and finds many applications in image processing. The first one (the region) is a geometric insight that can be used to more advanced image-parser techniques. Domains for tension fields allow a natural connection between geometry, mathematics, and optimization, which can be exploited for the design of advanced image processing tools like edge preserving, smoothing, and shape extraction.

4. Application of $\alpha-$tension field in image processing

This section aims to investigate and emphasizes the innovative aspects of the α-tension field as an operator in image processing, defined by:

$$\tau_\alpha(I) := (\alpha - 1)(1+ \mid \nabla I \mid^2)^{\alpha-2}\nabla I(\nabla \mid \nabla I \mid^2) + (1+ \mid \nabla I \mid^2)^{\alpha-1}\Delta(I), \quad (15)$$

with a specific focus on the case where $\alpha = 2$. For this particular value, the equation simplifies to:

$$\tau_2(I) = (1+ \mid \nabla I \mid^2)\Delta I + \nabla I(\nabla \mid \nabla I \mid^2). \quad (16)$$

In the remainder of this paper, the term $\tau_2(I)$ will be referred to as the *2-tension field*.

The 2-tension field is innovative because it possesses an architectural design that enables the trade-off between noise suppression and preservation of essential image characteristics (like edges, textures, or fine details). Unlike traditional methods like total variation regularization or anisotropic diffusion, which get compromised by the staircasing effect or by oversimplifying the gradients of structural complexity, this field is capable of incorporating higher- order statistics through the term $\nabla I(\nabla \mid \nabla I \mid^2)$. Such adaptation enables the model to respond to variations in

gradient strength while reducing artifact coverage as it propagates through low-transition detail and complex structure in the image.

Additionally, the theory of α-tension field is built on differential geometry as it is consistent with the geometric variational principles. This grounding sets it apart from heuristic approaches, bolstering its adaptive and versatile nature with a rigorous mathematical basis. In focusing on these characteristics—adaptability, flexibility, and mathematical robustness—we show that $\alpha-$tension field is not only solves the current challenges in areas such as image denoising, edge preservation, and feature enhancement but also sets the stage for new applications in medical imaging.

In the following, we further highlight the fundamental building blocks of this equation in the context of image processing, importance in solving primary tasks, mathematical properties, and the utility of it is overed in different image analysis tasks. This exploration highlights the potential impact of $\alpha-$tension field on image processing research and related fields.

4.1. Image denoising

In image processing, image denoising is a basic activity of eliminating undesired noise from an image, while at the same time keeping the significant structural details intact, such as edges, textures, and fine details.[18,19] The 2-tension field provides a sophisticated framework for achieving this balance. The factor $(1+\mid \nabla I \mid^2)\Delta I$ in (16), acts as a diffusion operator, which dynamically depends on the sharpness of the image, characterized by the local gradient magnitude $\mid \nabla I \mid$.[10] In those areas where the gradient magnitude is small, indicating smooth or homogeneous areas, the diffusion coefficient $(1+\mid \nabla I \mid^2)$ becomes approaching to unity, which encourages isotropic smoothing. This preserves flat regions without introducing artifacts. Nevertheless, such diffusion is inhibited at areas of high gradient, e.g., edges or abrupt transitions, thus preventing critical features from being blurred during the denoising procedure.

The second term $\nabla I(\nabla \mid \nabla I \mid^2)$ in (16), adds higher-order gradient information to the denoising process, making the $\tau_2(I)$ even more adaptive. This term guarantees that the evolution of the image intensity I will be determined not just by the local gradient, but also by the spatial fluctuation of gradient magnitude. Including this extra information allows the $\tau_2(I)$ to maintain small-scale details and edges that are often erased by simpler denoising models. The latter is particularly important in areas with texture where gradients change rapidly, where we want to preserve these details instead of oversmoothing them. The combined influence of the two terms in the (16) captures a trade-off between smoothing and sharpness, which is crucial for tasks where the goal is noise reduction while retaining relevant features.

4.2. Edge preservation

Edges are important features of images, because they usually contain the information of object boundary, structural characteristics, and semantic details of the image, so it is crucial to preserve that information in appropriate image processing algorithms. Through its nonlinear dependence on the magnitude of the gradient $\mid \nabla I \mid$, the 2-tension field maintains edges.[11] In particular, the term $(1+\mid \nabla I \mid^2)$ controls the diffusion by reducing the influence of the Laplacian operator ΔI where the gradient is high, i.e., on edges or regions with sudden transitions. Thus, this decrease in diffusion prevents the sharpening of edges, creating a crisp, and distinct visual without the uncertainties that the linear diffusion models induce. The 2-tension field effectively balances the trade-off between noise suppression and the preservation of important structural information by adaptively varying the degree of diffusion according to the local gradient information.

The term $\nabla I(\nabla \mid \nabla I \mid^2)$ in (16) provides additional edge preservation by integrating higher-order gradient information for the evolution of the image intensity I.[16,20] This term provides more control over the evolution of the gradient magnitude $\mid \nabla I \mid$ within the processing to further stabilize the edge structures. Such distributions have the property of retaining variations, so in areas where the gradient magnitude varies tremendously, for example, across object borders. This term ensures that the evolution of I accommodates these alterations so that fine-scale attributes do not get smoothed out. In applications, such as medical imaging, the ability to preserve edges can greatly suggest the quality of the reconstructed image. The combination of the two terms in (16) acts synergistically, resulting in edges being preserved and even enhanced, thereby making them more resilient to noise and other distortions.

4.3. Feature enhancement

The 2-tension field can be used to enhance the particular structures of an image, like edges, ridges, corners, and textures. Feature amplification is done by increasing the gradients of the region of interest while reducing the noise and irrelevant detail. $(1+\mid \nabla I \mid^2)\Delta I$ is a term employed to make sure that diffusion changes based

on the direction of the gradient, which means increased smoothing takes place in homogeneous regions and edges are preserved.[12,21] On the other hand, the second term, $\nabla I(\nabla \mid \nabla I \mid^2)$, puts the information of higher- order gradient into the evolution process. The term increases the contrast in the backgrounds with different gradient magnitudes, allowing finer features to be perceived more clearly. These mechanisms work in conjunction to preserve fine structural features while avoiding excessive smoothing and distortion of the image. The 2-tension field for feature enhancement has numerous practical applications, including for medical imaging. To give an example, in medical imaging, highlighting anatomical structures (blood vessels, tumors, or tissue boundaries) can improve the possibility of making an appropriate diagnosis significantly. This enables the 2-tension field to boost even weak or low-contrast features, which assist radiologists in identifying irregularities based on selective enhancement of gradients existing in such areas.

4.4. Numerical implementation and computational considerations

The code to numerically approximate the PDE $\tau_2(I)$ will then involve the discretization of the 2-tension field, so as to find an approximate solution on the computational grid. Common numerical discretization techniques, such as finite differences and finite elements, approximate continuous derivatives with discrete counterparts. For example, the Laplacian term ΔI can be approximated by means of second-order central differences, and at the same time the gradient terms $\mid \nabla I \mid$ and $\nabla \mid \nabla I \mid^2$ are traditionally calculated with first-order differences. Even since the 2-tension field is nonlinear because of terms including $(1+ \mid \nabla I \mid^2)$ and $\nabla I(\nabla \mid \nabla I \mid^2)$, one often uses iterative methods such as explicit or semi- implicit schemes.[15] Explicit methods update the image intensity I directly at each time step, but their stability may depend on very small time steps. The semi-implicit schemes will treat some terms implicitly, thus allowing for larger time steps which gives better computational efficiency while maintaining stability.

Due to the fact that the $\alpha-$tension field is nonlinear, a critical challenge when approximating this field numerically is ensuring stable and accurate results. The diffusion coefficient $(1+ \mid \nabla I \mid^2)$ is space- and time-varying, which if not treated well, can introduce instabilities.[13,22] This can be mitigated by adaptive time-stepping techniques as follows: the procedure used where size of time step is changed dynamically to capture local behavior of the solution. Numerical oscillations would be suppressed by regularization techniques, acting to smooth a tight jump in $\mid \nabla I \mid$. Another important aspect is the type of boundary conditions must be compatible with the physical interpretation of the problem. Thereby, conservation properties, for example, Neumann boundary conditions (zero gradient at the boundary) are commonly used in image processing to avoid artificial segments of features at the boundaries of the image domain.[15]

4.5. Comparison with existing methods

Notably, the $2-$tension field proposed in (16) provides major benefits compared to classical image processing methods like total variation (TV), regularization, and anisotropic diffusion. Its adaptivity is one such advantage due to the factoring of $(1+ \mid \nabla I \mid^2)$. This term interpolates the local diffusion strength according to local gradient magnitude $\mid \nabla I \mid$. On the other hand, regularization on traditional TV is frequently achieved with a fixed or piece-wise-linear weighting scheme, which might not sufficiently respond to the variable structure of the image. While for instance TV regularization is good in keeping sharp edges, it has the drawback of producing a staircasingeffect in smooth areas because it uses first-order gradients only. The 2-tension field improves this by adding higher-order information through $\nabla I(\nabla \mid \nabla I \mid^2)$ term to provide a more balanced approach between smoothing and edge conservation.[23] Such adaptivity preserves fine details like textures and subtle transitions without producing artifacts.

A novel aspect of the $\alpha-$tension field comes from its capability to encode higher-order gradient information, that is otherwise not taken into consideration by most simple models, such as anisotropic diffusion or TV-based methods. $\nabla I(\nabla \mid \nabla I \mid^2)$ contains the spatial variation of the gradient-magnitude explicitly, which can lead the model to respond to second order changes of the image intensity.[14,24] This is especially useful in cases where preserving or enhancing fine-scale structures (like ridges or corners) for improved segmentation is ideal. For example, in medical imaging, where delicate anatomical structures are of utmost diagnostic significance, including higher-order terms ensures that such details are not smoothed out during denoising. In contrast, many popular existing methods use only first-order derivatives, causing them to produce a less realistic model of complex structures. The interpretation in terms of the 2-tension field illustrates a more rigorous theoretical background of

this method, providing links to variational principles from geometry that tend to favor structural fidelity.

5. Comparison between tension field and $\alpha-$tension field in image processing

In this section, we compare the tension field to the nonlinear α-tension field with $\alpha = 2$, referred to as the 2-tension field. This comparison is a lens on the math formulations, properties, and usages in image processing. The behavior of each operator is illustrated in a figure to further clarify this comparison. After this, we display the algorithm that is used to make a comparison between the tension field and the 2-tension field of a 2D image.

Equation (7) demonstrated that tension field of 2D image I satisfies $\tau(I) = \Delta(I)$, where Δ is the Laplacian operator. This field is crucial for recognizing rapid intensity changes (edges, corners). The tension field is useful to highlight such running levels; however, it suffers from one major flaw, which is its high sensitivity toward the uniform regions, thereby making it prone to noise. This problem occurs because the tension field infers isotropic smoothing across the whole image pixel-wise, failing to differentiate between the actual substantive parts of the image and simple noise. Thus, while the tension field is good at basic edge detection, it can fail to find a balance between preserving important features while eliminating unwanted artifacts when used alone.

In contrast, the 2-tension field defined in equation (16) takes it a step further with the use of higher-order terms, allowing it to dynamically throttle the tension field according to the gradient norm $\mid \nabla I \mid$. The first term of (16) dynamically adjusts the diffusion coefficient based on the local gradient magnitude, and the second term incorporates higher-order gradient information. This inherently adaptive process protects those regions with high-edge structures, thus retaining their structural integrity. This minimizes the risk of over-smoothing in areas where noisy images are, while also letting through areas that are less affected (i.e., relatively smooth) in order to help smooth out the final image. Through an intelligent trade- off between these effects, the 2-tension field achieves the best performance across both feature preservation and noise cancellation tasks.

Adaptive modulation can be very significant for practical applications such as medical imaging. In this use case, it is important to retain fidelity in fine-scale structures and edges, which typically contain valuable diagnostic or interpretive information. As an example, in the medical imaging field, the subtle anatomical features in the image (i.e., blood vessels or tissue boundaries) need to be preserved and no artifact should be introduced in the denoising process. Additionally, the term $\nabla I(\nabla \mid \nabla I \mid^2)$ in the 2-tension field illustrates how the higher-order gradient information can be integrated. This minute change, which reacts to linear differences in the strength of the gradient, is what enables the model to automatically amplify or damp specific features so that the native image structure is maintained while still considering the issue of noise.

The strong mathematical background of the 2-tension field is shown from a theoretical point of view by the connection between the 2-tension field and geometric variational principles. This provided a framework, which naturally balances smoothness with structure accuracy (key for good image processing), as can be seen in Figure 2. In contrast to traditional methods, which rely on static or piecewise -linear weighting techniques, the 2-tension field reacts according to the spatial characteristics of the image, proving versatile and adaptable in differing scenarios. By dynamically adjusting based on local conditions, such as textures and other fine transitions, it can provide high efficiency with no unwanted artifacts. Moreover, the versatility of the equation allows it to be tailored for particular applications, such as medical imaging, where preserving fine details is critical. In brief, the 2-tension field represents a significant leap in image processing, providing computationally speedy solution for denoising, edge retention, and features enhancement tasks.

Figure 2 consists of eight images that illustrate, step by step, how the tension field and each term of the 2-tension field are applied to the input image. It also compares the performance of the tension field and the 2-tension field on a well-known benchmark in image processing, highlighting their respective strengths and limitations. Image (a_1) is the original image used as input for both operators. Some features of $\mid \nabla I \mid^2$ are demonstrated in Image (a_2) which influences edge detection. On the other hand, Image (b_1) shows the output of the tension field as it not only efficiently detects edges but also amplifies noise in smooth regions due to its isotropic smoothing properties. To explore the 2-tension field indepth, we evaluate every term of $\tau_2(I)$ and show

their effects. Images (b_2) and (c_1) show the directional gradients retrieved from Sobel-X and Sobel-Y, respectively, which store horizontal and vertical edge details. The first term $(1+ \mid \nabla I \mid^2)\Delta I$ output is shown in Image (c_2) that highlights for edges while suppressing diffusion at flat areas. This is done by controlling the diffusion process using adaptive modulation by the gradient magnitude, preserving, or smoothing around edges. The second term $\nabla I(\nabla \mid \nabla I \mid^2)$ captures higher- order features of the image, detecting corners, junctions, and fine details of the image. It does this by capturing higher-order gradient information that helps to understand the local structures and spatial variations present in the image. Visualizing the result of this term (Image (d_1)) shows its power to detect and amplify these tiny features. Lastly, Image (d_2) demonstrates briefly the effect of combining all these to compute the final output, which is $\tau_2(I)$ and we can see clearly that it retains the structure while sufficiently filtering the noise. The extensivity of the deconstructions performed in this talk shows the virtue of the α-tension field, and its extreme robustness for high-level image processing tasks of delicate detail preservation and artifact suppression.

Step-by-step analysis of the Figure 2 describes different interactions of 2-tension field equation components: the tension field operator $\tau(I)$ is the edge detector operator. It has high values on the edges but tends to also amplify noise due to its isotropic smoothing nature. To overcome this drawback, in the definition of $\tau_2(I)$, the term $1+ \mid \nabla I \mid^2$ controls the weight of the Laplacian, with features being promoted and noise being suppressed through the gradient term. The second term $\nabla I(\nabla \mid \nabla I \mid^2)$ accounts for how the gradient magnitude changes in space, allowing for more adaptability and specificity when extracting features from complex structures like corners or junctions. Thus, by combining these two terms together, the 2-tension field is capable of preserving significant details while getting rid of undesired artifacts, leading to better image processing results.

Algorithm 2 presents the pseudocode that outlines the detailed implementation procedure for both the tension field and the 2-tension field, as illustrated in Figure 2. It starts with computing the gradient components, that is, ∇I_x and ∇I_y using the central differences method, and finally computing the gradient $\mid \nabla I \mid$. This is followed by applying the baseline tension field via the Laplacian operator (ΔI), which can also detect edges well but introduces noise amplification in smooth areas due to its isotropic smoothing characteristics. We compute two main terms for the 2-tension field, the first one describes a weighted diffusion process $(1+ \mid \nabla I \mid^2)\Delta I$, which depends on the structure of the image, presenting low diffusion of small magnitudes and preserving the integrity of edges. The second term, $\nabla I(\nabla \mid \nabla I \mid^2)$, incorporates higher-order gradient information, which further improves the preservation of complex structures like edges or corners. Through the addition of these two terms, one can arrive at the final output of the 2-tension field which attains a certain balance between noise reduction and detail preservation. Moreover, the output for each step is plotted to give clarity on how the operators affect the image across its stages, from basic edge detection to complex feature extraction.

Comparison between tension field and 2-tension field in different aspects is represented in Table 1. Although the tension field is linear, computationally simple, and works well for simple edge detection, it is also very sensitive to noise because of the isotropic smoothing and second derivatives because it can artificially inflate noise in flat parts. On the other hand, the 2-tension field is non-linear and includes adaptive modulation that uses magnitude of gradient to modulate the 2-tension field, which allows it to enhance edges and prevent noise amplification. The anisotropic smoothing behavior of this approach preserves edges in high-gradient regions while smoothes homogeneous areas, making it more robust to noise. For advanced image processing problems like denoising, edge-preserving, smoothing, and feature enhancement, the 2-tension field with its higher-order gradient terms is more suitable, especially for tasks where the preservation of fine details is critical and the problems better approximate the concept of artifacts.

To sum up, this section has discussed the classical tension field and 2-tension field in the sense of image processing and their merits and drawbacks. The tension field $\tau(I) = \Delta I$, which has the property of solving isotropic smoothing, is a very good edge detector, but the linearity and the second gradients behavior of this operator will made it very sensitive to noise, especially in homogeneous zones. On the other hand, the 2-tension field takes into account higher-order gradient hints and modulates diffusion based on such local gradients adaptively. This adaptive behavior both minimizes amplification of deleterious noise as well as allowing crucial traits such

(a_1) Original image.

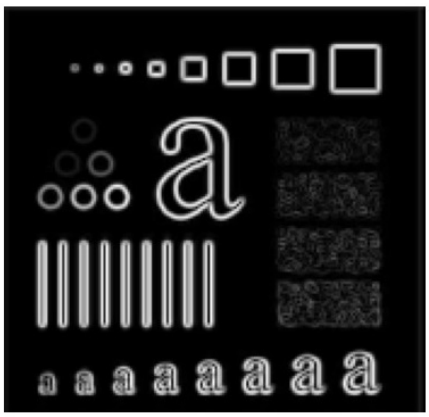

(a_2) The effect of $\mid \nabla I \mid^2$.

(b_1) The effect of tension field.

(b_2) The effect of Sobel X.

(c_1) The effect of the Sobel Y.

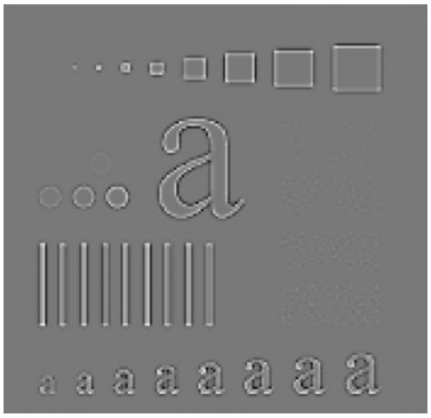

(c_2) The effect of $(1+ \mid \nabla I \mid^2)\Delta I$.

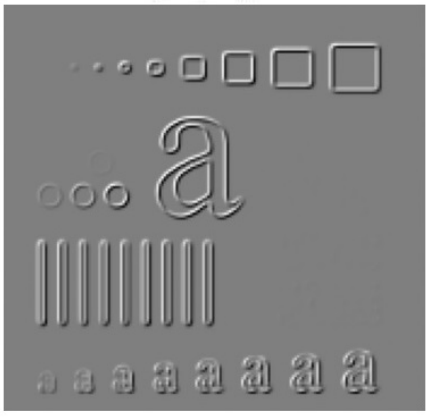

(d_1) The effect of $\nabla I(\mid \nabla I \mid^2)$.

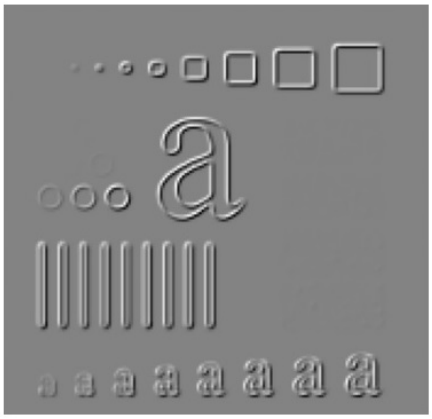

(d_2) The effect of $\tau_2(I)$.

Figure 2. Evaluating the strengths and limitations of tension field versus 2-tension field in edge detection and noise suppression.

Algorithm 2 The algorithm used to compare the performance of the tension field and 2-tension in Figure 2.

Require: Original image I
Ensure: Output images demonstrating the effects of the tension field and α-tension field

Load the original image I.
Store this as (a_1): Original image.
Compute the gradient magnitude $|\nabla I|^2$ using:

$$|\nabla I|^2 = (\partial_x I)^2 + (\partial_y I)^2$$

where $\partial_x I$ and $\partial_y I$ are partial derivatives in the x- and y-directions, respectively.
Store this as (a_2): Gradient magnitude visualization.
Compute the output of the tension field:

$$\tau(I) = \Delta I$$

where ΔI is the Laplacian of I.
Store this as (b_1): Tension field output.
Compute Sobel-X ($\partial_x I$) and Sobel-Y ($\partial_y I$) gradients:
(b_2): Horizontal edge details (Sobel-X).
(c_1): Vertical edge details (Sobel-Y).
Compute the first term of the α-tension field:

$$T_1 = (1 + |\nabla I|^2)\Delta I$$

where $|\nabla I|^2$ controls adaptive diffusion.
Store this as (c_2): Visualization of the first term.
Compute the second term of the α-tension field:

$$T_2 = \nabla I \cdot (\nabla |\nabla I|^2)$$

where $\nabla |\nabla I|^2$ captures higher-order gradient information.
This term detects corners, junctions, and fine details.
Store this as (d_1): Visualization of the second term.
Combine terms to compute the α-tension field for $\alpha = 2$:

$$\tau_\alpha(I) = T_1 + T_2$$

where:
$T_1 = (1 + |\nabla I|^2)\Delta I$,
$T_2 = \nabla I \cdot (\nabla |\nabla I|^2)$.
Store this as (d_2): Final output of the α-tension field.
Compare results:
Tension field (b_1): Efficient edge detection but amplifies noise.
α-Tension field (d_2): Retains structure while filtering noise effectively.
Summary of outputs:
(a_1): Original image.
(a_2): Gradient magnitude $|\nabla I|^2$.
(b_1): Tension field output.
(b_2): Sobel-X gradient.
(c_1): Sobel-Y gradient.
(c_2): First term of α-tension field.
(d_1): Second term of α-tension field.
(d_2): Final α-tension field output.

as edges, corners, and fine details to be conserved and even accentuated. The magnitude of the 2-tension field makes the algorithm highly flexible when it comes to more advanced functionalities, including denoising, edge-preserving, smoothing, and feature enhancement, all of which are highly desirable in areas such as medical imaging or wherever structural integrity is important. The first term of this equation regulates the diffusion, relying on the spatial change and suppression of diffusion in the regions of high gradients to preserve the edges, while the second term keeps the

Table 1. Comparison of key characteristics between tension field and 2-tension field.

Aspect	**Tension Field**	**2-Tension Field**
Linearity/Nonlinearity	Linear	Nonlinear
Edge detection	Highlights edges but may amplify noise	Enhances edges adaptively, reducing noise amplification
Noise sensitivity	High sensitivity to noise due to second derivatives	Less sensitive to noise due to adaptive modulation
Smoothing behavior	Isotropic smoothing	Anisotropic smoothing: preserves edges while smoothing within homogeneous regions
Complexity	Simple and computationally efficient	More complex due to additional terms involving gradient magnitudes
Use cases	Suitable for simple edge detection or preprocessing steps	Ideal for advanced image processing tasks like denoising, edge-preserving smoothing

Table 2. Overview of the experimental setup.

Dataset	Noise Variance	Samples	Repetitions	Experiments
LIDC-IDRI	0.01	40	10	400
	0.05	40	10	400
	0.1	40	10	400

spatial diversity in the magnitude of the gradient itself, thus seriously contributing to the stabilization and enhancement of high-resolution structures. In numerical implementation, stability and computational efficiency are achieved through the use of finite differences and iterative methods. In summary, the 2-tension field represents a significant leap forward compared to traditional methods, as it offers a mathematically sound and flexible approach to surmount the smoothness-structural preservation trade-off in a variety of image processing tasks.

5.1. 2-Tension versus tension field operator: Gaussian noise reduction in medical imaging

This part is dedicated to comparing two noise reduction methods–the 2-tension field operator and the tension field operator–in terms of how much Gaussian noise is diminished. This comparison is carried out on the lung CT images for cancer detection in the LIDC-IDRI Dataset.[8]

Stratified random sampling was used to obtain a representative and diverse sample.[25] Forty images were randomly sampled from the LIDC-IDRI dataset, with cases of mixed nodule complexity. Each image was corrupted with three amounts of Gaussian noise with variances of 0.01, 0.05, and 0.1. To maintain consistency for evaluation, each experiment was repeated independently a total of 10 times. Structural Similarity Index Measure (SSIM) was used to assess the quality of the image restoration after denoising.[26]

Table 3 provides an overview of the experimental setup.

Table 3 compares two denoising methods (the 2-tension field operator and the tension field operator) on the LIDC-IDRI dataset at three different Gaussian noise levels (variance = 0.01, 0.05, 0.1). The methods are compared based on SSIM scores to determine which denoising method preserves the structural similarity after reducing noise levels. For the lower noise levels (variance = 0.01), the 2-tension field operator had a slightly better performance than the tension field operator (SSIM values = 0.93 vs. 0.92). As noise variance increases (variance = 0.05 and 0.1), the 2-tension field operator continued to show better performance than the tension field operator (SSIM values = 0.87 vs. 0.85 and 0.81 vs. 0.76). These results show that the 2-tension field operator has an increased robustness factor, which preserves structural integrity under higher noise conditions than the tension field operator.

Table 3. SSIM scores for the LIDC-IDRI Dataset

Noise Variance	2-Tension SSIM	Tension SSIM
0.01	0.93	0.92
0.05	0.87	0.85
0.1	0.81	0.76

In summary, the comparative study shows the 2-tension field operator to be a powerful, generative method for removing Gaussian noise in medical imaging modalities. To weight these findings, rigorous statistical approaches have been implemented. Stratified sampling provided variability and representativeness and a number of trials (10 per image and noise level) provided test-retest reliability. These methodological steps ensure that SSIM values reported here are valid and repeatable. In general, this study provides helpful context for understanding the relative performance of these denoising techniques, which will be helpful for future application in medical imaging.

6. Conclusions and future research directions

The α-tension field with $\alpha = 2$, well-known as 2-tension field and defined in (16), is a substantial work in image analysis. Because it does a good job of balancing contradictory objectives like noise suppression, edge preservation, and feature enhancement. So, this field is very powerful because it adapts itself to the local characteristics of the image and manages to denoise smooth regions effectively while keeping edges and fine features sharp. This adaptivity is a consequence of the nonlinear dependency of the evolution rates on the gradient magnitude $\mid \nabla I \mid$, which changes the diffusion according to the local geometry of the image. As a result, the $2-$tension field is particularly well suited for tasks where maintaining the structural integrity of the original geometry is important, such as in medical imaging and remote sensing applications, among others.

Notably, the 2-tension field comes from geometric variational principles. This correspondence also gives a more solid background for understanding the behavior of the 2-tension field and its success in image processing. The mathematical aspect underscores how the 2-tension field finds a compromise between regularization (smoothing) and fidelity to the original image structure. Integrating higher-order information of the gradient with the term $\nabla I(\nabla \mid \nabla I \mid^2)$ allows the 2-tension field to provide a richer structure of the images compared to prior approaches such as total variation (TV) regularization or linear diffusion. This provides deeper theoretical underpinnings that help with parameter selection while also forming the basis for the construction of robust numerical schemes.

In practice, the 2-tension field is applied in many imaging tasks, such as denoising (for noise removal) and edge preservation (for interpolation filling). It can be applied to usecases like image inpainting (filling in missing or corrupted regions), segmentation (identifying and delineating objects in an image), and so on. These more adaptive diffusion mechanisms aid in the model's performance in both the fine textures present in satellite imagery and the necessary edge boundaries present in biomedical scans. In addition, integrating local image features into the diffusion process allows for a diffusion process that can adjust based on the level of detail within the image, making this approach highly effective for use in scientific as well as industrial applications.

The α-tension field operator demonstrates significant potential for future applications in remote sensing image processing. While this study primarily focuses on its effectiveness in medical imaging tasks such as denoising and edge preservation, the inherent properties of the α-tension field–such as its nonlinear adaptability, sensitivity to local gradient magnitudes, and ability to preserve fine structural details while reducing noise–make it a promising candidate for handling large-scale and complex remote sensing data. Remote sensing images often suffer from atmospheric interference, sensor noise, and varying illumination conditions, where maintaining spatial and textural integrity is crucial for accurate interpretation and analysis.[12] The α-tension field offers a geometrically grounded, robust framework that can be adapted to address these challenges effectively. Future research may explore optimized numerical implementations, adaptive parameter selection (e.g., through machine learning), and integration with real-time processing pipelines, making the α-tension field a valuable tool for next-generation remote sensing applications such as environmental monitoring, urban planning, and disaster response systems.

Acknowledgments

None.

Funding

None.

Conflict of interest

The authors declare that they have no conflict of interest regarding the publication of this article.

Author contributions

Conceptualization: Amin Jajarmi, Seyyed Mehdi Kazemi Torbaghan
Investigation: Amin Jajarmi, Yaser Jouybari Moghaddam

Methodology: Seyyed Mehdi Kazemi Torbaghan, Yaser Jouybari Moghaddam
Formal analysis: Seyyed Mehdi Kazemi Torbaghan, Amin Jajarmi
Writing – original draft: Seyyed Mehdi Kazemi Torbaghan
Writing – review & editing: Amin Jajarmi

Availability of data

Not applicable.

References

1. Kazemi Torbaghan SM, Salehi K, Babayi S. Existence and stability of α-harmonic maps. *J Math.* 2022;2022(1):1906905.
2. Sacks J, Uhlenbeck K. The existence of minimal immersions of 2-spheres. *Ann Math.* 1981;113(1):1-24.
3. Shahnavaz A, Kazemi Torbaghan SM, Kouhestani N. Sacks-Uhlenbeck α-harmonic maps from Finsler manifolds. *J Finsler Geom Appl.* 2024;5(2):70-86.
4. Lamm T, Malchiodi A, Micallef M. A gap theorem for α-harmonic maps between two-spheres. *Anal PDE.* 2021;14(3):881-889.
5. Li J, Zhu X. Energy identity and necklessness for a sequence of Sacks–Uhlenbeck maps to a sphere. *Ann Inst Henri Poincaré (C) Anal Non Lineaire.* 2019; 36(1):103-118.
6. Shahnavaz A, Kouhestani N, Kazemi Torbaghan SM. The Morse index of Sacks–Uhlenbeck α-harmonic maps for Riemannian manifolds. *J Math.* 2024;2024(1):2692876.
7. Perelman G. Finite extinction time for the solutions to the Ricci flow on certain three-manifolds. arXiv Preprint Math/0307245; 2003.
8. `https://www.kaggle.com/datasets/zhangweiled/lidcidri`
9. Kazemi Torbaghan SM, Jouybari Y. Generalized harmonic maps and applications in image processing. *J Finsler Geom Appl.* 2025;6(1):23-35.
10. Birkfellner W. Applied Medical Image Processing: A Basic Course. CRC Press; 2024.
11. Wei W, Zhou B, Polap D, Wozniak M. A regional adaptive variational PDE model for computed tomography image reconstruction. *Pattern Recogn.* 2019;92:64-81.
12. Canty MJ. Image Analysis, Classification and Change Detection in Remote Sensing: With Algorithms for Python. CRC Press; 2019.
13. Oprea J. Differential Geometry and its Applications. American Mathematical Society; 2024.
14. Tian C, Chen Y. Image segmentation and denoising algorithm based on partial differential equations. *IEEE Sens J.* 2019;20(20):11935-11942.
15. Kimmel R. Numerical Geometry of Images: Theory, Algorithms, and Applications. Springer Science & Business Media; 2012.
16. Sapiro G. Geometric Partial Differential Equations and Image Analysis. Cambridge University Press; 2006.
17. Heijmans HJ. Mathematical morphology: a modern approach in image processing based on algebra and geometry. *SIAM Rev.*, 1995;37(1):1-36.
18. Chaudhari DJ, Malathi K. Detection and prediction of rice leaf disease using a hybrid CNN-SVM model. *Opt Mem Neural Netw.*, 2023;32(1):39-57.
19. Kuijper A. Geometrical PDEs based on second-order derivatives of gauge coordinates in image processing. *Image Vis Comput.* 2009;27(8):1023-1034.
20. Varanasi S, Malathi K. Self-improved COOT optimization-based LSTM for patient waiting time prediction. *Multimedia Tools Appl.* 2023;83(13): 39315-39333.
21. Babu VD, Malathi K. Three-stage multi-objective feature selection with distributed ensemble machine and deep learning for processing of complex and large datasets. *Measure Sens.* 2023;28: 100820.
22. Kumar MR, Malathi K. An innovative method in classifying and predicting the accuracy of intrusion detection on cybercrime by comparing decision tree with support vector machine. In: *2022 International Conference on Business Analytics for Technology and Security (ICBATS)*, Dubai; 2022.
23. Duits R, Citti G, Fuster A, Schultz T. Differential geometry and orientation analysis in image processing. *J Math Imaging Vis.* 2018;60:763-765.
24. Rambabu V, Malathi K, Mahaveerakannan R. An innovative method to predict the accuracy of phishing websites by comparing logistic regression algorithm with support vector machine algorithm. In: *6th International Conference on Electronics, Communication and Aerospace Technology*, Coimbatore; 2022.
25. Kumar A, Bhushan S, Mustafa MS, Aldallal R, Aljohani HM, Almulhim F A. Novel imputation methods under stratified simple random sampling. *Alexandria Eng J.* 2024;95:236-246.
26. Reznik Y. Another look at SSIM image quality metric. *Electron Imaging.* 2023;35: 1-7.

Seyyed Mehdi Kazemi Torbaghan *Seyyed Mehdi Kazemi Torbaghan received his B.Sc. in Mathematics from the University of Birjand, Iran, in 2009, and his M.Sc. and Ph. D. degrees in differential geometry from Amirkabir University of Technology (Tehran Polytechnic) in 2012 and 2017, respectively. Currently, he is an Assistant Professor in the Department of Mathematics, University of Bojnord, Iran. His research interests include differential geometry, image processing, game theory, and mathematical modeling.*
`https://orcid.org/0000-0002-7150-1705`

Yaser Jouybari Moghaddam *Yaser Jouybari Moghaddam received his B.Sc. in Surveying Engineering from the University of Isfahan, Iran, in 2012, and an M.Sc. and Ph. D. in Remote Sensing from the University of Tehran in 2014 and 2018, respectively. He is an Assistant Professor at the Department of Surveying Engineering, University of Bojnord, Iran. His research interests include machine learning, image processing, unmanned aerial vehicles (UAVs) and photogrammetry.*

https://orcid.org/0000-0001-5455-6352

Amin Jajarmi *Amin Jajarmi received his B.Sc., M.Sc., and Ph.D. in Electrical Engineering from Ferdowsi University of Mashhad in 2005, 2007, and 2012, respectively. He is currently an Associate Professor in the Department of Electrical Engineering at the University of Bojnord, Iran. His research interests include computational methods for optimal control of nonlinear and fractional-order systems, mathematical modeling with real-world applications, and chaos control and synchronization.*

https://orcid.org/0000-0003-2768-840X

An International Journal of Optimization and Control: Theories & Applications
(https://accscience.com/journal/ijocta)